

*To appear in “Magnetic Coupling between the Interior and the Atmosphere of the Sun”, eds. S. S. Hasan and R. J. Rutten, Astrophysics and Space Science Proceedings, Springer-Verlag, Heidelberg, Berlin, 2009.*

---

## Probability Density Functions to Represent Magnetic Fields at the Solar Surface

M. Sampoorna

Indian Institute of Astrophysics, Koramangala, Bangalore 560 034, India

**Summary.** Numerical simulations of magneto-convection and analysis of solar magnetogram data provide empirical probability density functions (PDFs) for the line-of-sight component of the magnetic field. In this paper, we theoretically explore effects of several types of PDFs on polarized Zeeman line formation. We also propose composite PDFs to account for randomness in both field strength and orientation. Such PDFs can possibly mimic random fields at the solar surface.

### 1 Introduction

Magneto-convection on the Sun has a size spectrum that spans several orders of magnitude and develops eddies with sizes much smaller than the spatial resolution of current spectro-polarimeters (about 0.2 arcsec or 150 km at the photospheric level). Thus the Stokes profiles that we observe are always averages over space, time, and along the line-of-sight (LOS). This suggests that it would be appropriate to characterize the magnetic field responsible for spectral line polarization by a probability density function (PDF). The case of Gaussian PDFs was studied by Dolginov & Pavlov (1972); Domke & Pavlov (1979); Frisch et al. (2005, 2006a,b, 2007); Sampoorna et al. (2008a). In this paper we study PDFs determined from observations by Stenflo & Holzreuter (2002, 2003a,b) and from magneto-convection simulations by Stein & Nordlund (2006, see also Vögler et al. 2005). Sampoorna et al. (2008b) used these PDFs to compute mean solutions in the macro and micro-turbulent limits. Macro and micro-turbulence are also referred to as optically thick and optically thin limits. In this paper we discuss in detail the mean solutions computed for a more general regime of meso-turbulence.

It is well known that photospheric photon mean free paths (50–100 km in the optical) correspond approximately to the sizes of meso-turbulent magnetic eddies. Calculation of mean Stokes parameters in this regime was considered by Landi degl’Innocenti (1994); Frisch et al. (2006b,a); Carroll & Staude (2003, 2005); Carroll & Kopf (2007). We use a Kubo-Anderson Process (KAP)

with correlation length  $1/\nu$  (where  $\nu$  is number of jumps per unit optical depth) and a PDF to characterize the random magnetic field (Frisch et al. 2006b). Using KAP in a Milne-Eddington model atmosphere, Frisch et al. (2006b) deduce explicit expressions for the mean and rms fluctuations of the emergent Stokes parameters. In this paper we use those expressions to compute mean solutions for magnetic eddies of arbitrary size.

## 2 Scalar PDFs

Recently Stenflo & Holzreuter (2002, 2003a,b) have found from an analysis of high resolution La Palma and MDI solar magnetograms that the PDF for the LOS component is nearly independent of the spatial scale and can be well represented by a Voigt function. This PDF has a Gaussian core (centered around zero field) with a magnetic width  $\Delta_B$ , and Lorentzian wings with a magnetic damping parameter  $a_B$ . The quantity  $\Delta_B$  is a measure of the rms fluctuations of the LOS component.

A Voigt PDF with  $\Delta_B = 6$  G and  $a_B = 1.5$  best fits the empirical PDF for LOS field strength derived from La Palma magnetograms. A symmetric Voigt function has zero net flux. In real magnetograms magnetic flux is locally unbalanced. Non-zero net flux can be generated by a Voigt PDF that has a symmetric core, but different  $a_B$  for positive and negative polarities.

Magneto-convection simulation near the solar surface by Stein & Nordlund (2006) show that the magnetic field is intermittent with a stretched exponential distribution. Here we restrict ourselves to asymmetric scalar PDFs as they represent the photospheric conditions better.

### 2.1 Asymmetric Voigt PDF

In terms of parameters  $a_B$  and  $\Delta_B$ , symmetric Voigt PDF has the form

$$P_V(y, a_B) = \frac{a_B}{\pi^{3/2}} \int_{-\infty}^{+\infty} \frac{e^{-u^2}}{(y-u)^2 + a_B^2} du. \quad (1)$$

In the above equation we have introduced non-dimensional parameters

$$y = B/\Delta_B, \quad u = B_1/\Delta_B, \quad \gamma_B = \Delta_B/B_D, \quad (2)$$

where  $1/B_D = ge/(4\pi mc\Delta\nu_D)$ , in standard notation. Here  $B$  is the random magnetic field component along a given direction, and  $\Delta\nu_D$  is the frequency Doppler width. Thus  $\gamma_B$  represents rms fluctuations  $\Delta_B$  converted to Zeeman shift in Doppler width units.

Asymmetric Voigt PDFs can be constructed by choosing different values of  $a_B$  for different parts of the PDF while keeping the Gaussian core symmetrical. Figure 1a shows examples of asymmetric PDFs (see Sampoorna et al.

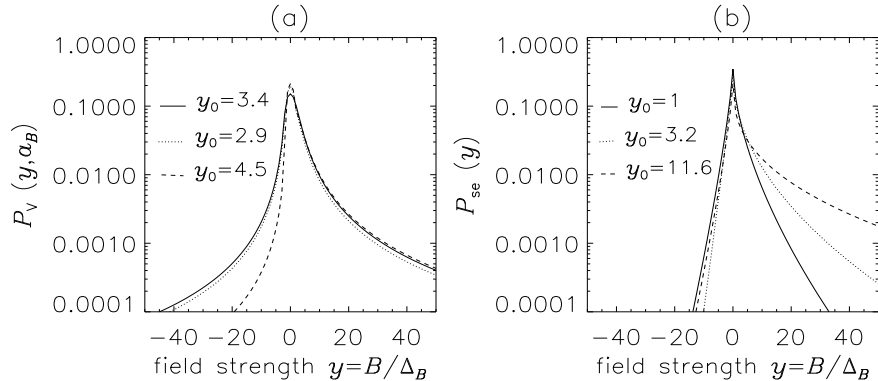


**Fig. 1.** (a) Asymmetric Voigt and (b) Stretched exponential PDFs. The  $y$ -scale is related to the  $B$ -scale through  $\Delta_B$  ( $= 6$  G according to Stenflo & Holzreuter 2002).

2008b, for details), which more or less resemble the PDF for the La Palma magnetogram shown in Fig. 2 of Stenflo & Holzreuter (2002). The mean magnetic field  $y_0$  is the average of  $y$  over  $P_V(y, a_B)$ .

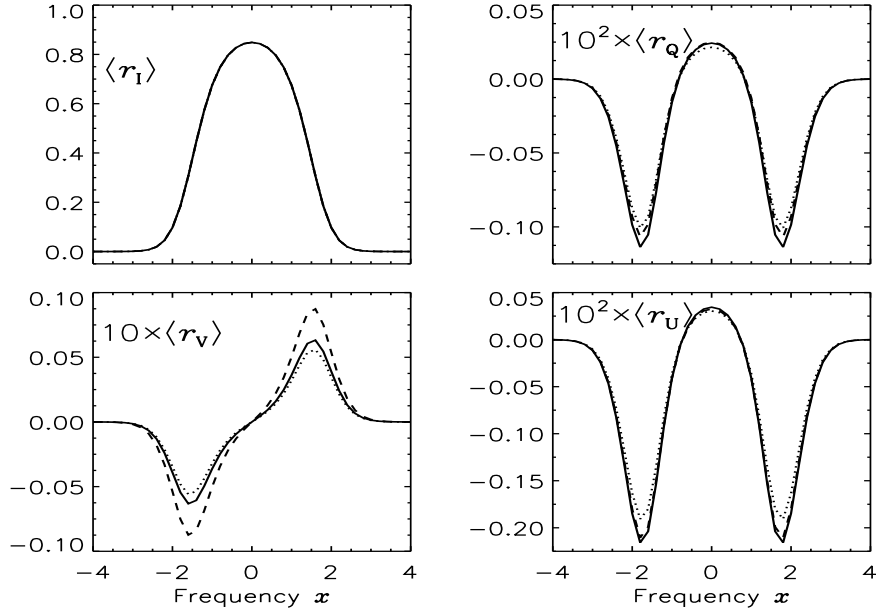
Mean emergent residual Stokes parameters  $\langle r_{I,Q,U,V} \rangle$  are computed using asymmetric scalar PDFs for magnetic eddies of arbitrary size. The random field has a fixed orientation with respect to the LOS defined by polar angles  $(\gamma, \chi) = (60^\circ, 30^\circ)$ . Emergent residual Stokes parameters are defined by  $r_I = [I_c - I]/C_1$  and  $r_X = -X/C_1$ , with the symbol  $X$  denoting  $Q, U$  or  $V$ . The constant  $C_1$  is the slope of continuum source function  $S(\tau_c) = C_0 + C_1\tau_c$ , with  $\tau_c$  the continuum optical depth. The continuum intensity at the surface is  $I_c = C_0 + C_1$ . This model has damping parameter  $a = 0$  and line strength parameter (ratio of line to continuum absorption coefficient)  $\beta = k_0/k_c = 10$ . We also assume that the spectral line has a wavelength around  $5000 \text{ \AA}$ , a Landé factor of 2 and a Doppler width of  $1.5 \text{ km s}^{-1}$ . For this typical line,  $B_D = 1.07 \times 10^3$  G. Hence  $\gamma_B = 0.0056$  for an rms magnetic field fluctuation  $\Delta_B = 6$  G. As a result the  $\langle r_I \rangle$  profiles in all figures in this paper remain insensitive to the PDF parameters.

Figure 2 shows  $\langle r_{I,Q,U,V} \rangle$  computed using the 3 PDFs in Fig. 1a for  $\nu = 5$ . Note that  $\langle r_V \rangle$  is zero if one uses a symmetric PDF with zero mean field. The  $\langle r_{Q,U} \rangle$  profiles show very small sensitivity to PDF asymmetry, while the  $\langle r_I \rangle$  profiles indeed are insensitive. For all three PDFs,  $\langle r_V \rangle$  peaks around  $x \approx 1.5$ . The peak amplitudes increase with the mean field.

## 2.2 Asymmetric stretched exponential PDF

A symmetric stretched exponential may be written in functional form as

$$P_{se}(y) dy = C e^{-|y|^k} dy. \quad (3)$$



**Fig. 2.**  $\langle r_{I,Q,U,V} \rangle$  computed with asymmetric Voigt PDFs in Fig. 1a for  $\nu = 5$ . Reference to line types is the same as in Fig. 1a.

The quantity  $k$  takes values between 0 and 1 and is referred to as the stretching parameter.  $C$  is the normalization constant.

We construct asymmetric stretched exponential PDFs with non-zero mean field by choosing different  $k$  values for positive and negative polarities. Figure 1b shows three examples (see Sampoorna et al. 2008b, for details).

Mean residual Stokes profiles computed with these three PDFs are shown in Fig. 3. For  $\nu = 5$ , we observe a clear increase in the peak amplitudes of  $\langle r_{Q,U,V} \rangle$  when the mean field  $y_0$  increases. However, the peak positions are essentially insensitive to  $y_0$ . The  $\langle r_I \rangle$  profiles remain insensitive to PDF asymmetry. Differences between the solutions for  $\nu = 5$  and the macro-turbulent limit appear for  $\langle r_{Q,U} \rangle$  when  $y_0 = 11.6$ , due to the extended tail of the PDF for positive polarities. For  $\langle r_V \rangle$ , the differences remain small even for  $y_0 = 11.6$ . The relative insensitivity of  $\langle r_V \rangle$  to the scale of magnetic field fluctuations has been observed for Voigt type PDFs (see Sampoorna et al. 2008b) and also for symmetric Gaussian PDFs with non-zero mean field (Frisch et al. 2006b). It is due to the fact that the PDF asymmetry is sharply peaked around  $y_0$ . In the limit of a Dirac distribution, there would be no difference between solutions for different  $\nu$  values since the magnetic field would be deterministic. It thus appears that a mean value of Stokes  $V$  can be calculated with reasonable confidence using the micro-turbulent limit, a remark made already in Frisch et al. (2006b).

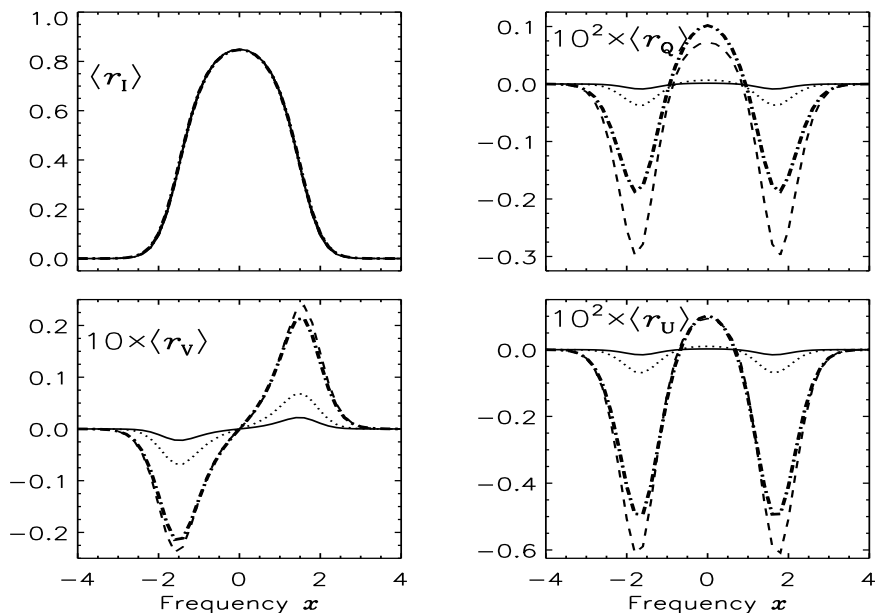


**Fig. 3.**  $\langle r_{I,Q,U,V} \rangle$  for asymmetric stretched exponential PDFs. Solid, dotted and dashed lines refer to  $\nu = 5$  (the same line types as in Fig. 1b). Heavy dot-dashed line refers to macro-turbulent limit for  $y_0 = 11.6$ .

### 3 Angular PDFs

A large fraction of the solar atmosphere is filled with mixed polarity fields, and the inter-granular lanes contain fields that are preferentially directed upward or downward. To represent this situation, we consider magnetic fields that have a fixed value of the strength  $B$  but random orientations. For such a random field, following angular distribution has been suggested by Stenflo (1987):

$$P_{\text{pl}}(\mu_B) = \frac{(p+1)}{4\pi} |\mu_B|^p, \quad -1 \leq \mu_B \leq +1. \quad (4)$$

Here,  $\mu_B = \cos \theta_B$ , with  $\theta_B$  the field orientation with respect to the atmospheric normal. The power law index  $p$  can take any value; the  $p = 0$  case corresponds to an isotropic distribution. As  $p$  increases the distribution becomes more and more peaked in the vertical direction.

Mean profiles  $\langle r_{I,Q} \rangle$  are calculated for  $\nu = 5$ , magnetic field strength  $B/B_D = 0.1$ , line strength  $\beta = 10$ , damping parameter  $a = 0$ , and the power law index  $p$  a free parameter. Figure 4 shows  $\langle r_{I,Q} \rangle$  at the limb ( $\mu = 0.1$ ). A comparison of this figure with Fig. 12 of Sampoorna et al. (2008b) computed for the micro-turbulent limit shows that there is very little difference between the two. This is because the absolute value of the magnetic field along the LOS is bounded by the condition  $B/B_D = 0.1$ . Since the field is weak,  $\langle r_Q \rangle \ll \langle r_I \rangle$ .

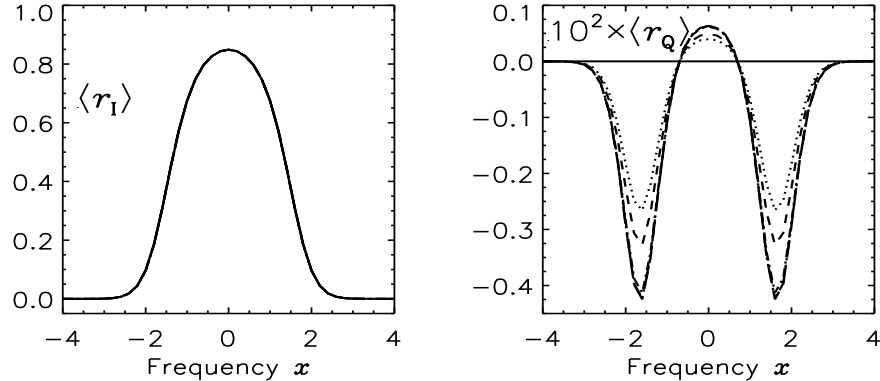


**Fig. 4.**  $\langle r_{I,Q} \rangle$  at  $\mu = 0.1$  (limb observation) computed for  $\nu = 5$  and angular power law PDF (Eq. (4)). Line types:  $p = 0$  (solid), 5 (dotted), 10 (dashed), 100 (dot-dashed), 500 (dash-triple-dotted), and 1000 (long dashed). In this case  $\langle r_{U,V} \rangle = 0$ .

Further,  $\langle r_Q \rangle$  is zero for  $p = 0$ . As  $p$  gets larger,  $\langle r_Q \rangle$  first increases with  $p$  and then saturates for  $p \simeq 100$  (see Fig. 4).

#### 4 Vector magnetic field distributions

To describe a random vector magnetic field we need a PDF that simultaneously accounts for strength and angle fluctuations. *From physical considerations one may argue that angular variation should be strongly field-strength dependent* (see de Wijn et al. 2009). For the strongest fields the distribution should be peaked around the vertical direction, as strong fields tend to have intermittent fluxtube morphology. The weakest fields on the other hand would be passively moved and bent by turbulent fluid motions and so get so tangled up that their distribution would be nearly isotropic. The transition from isotropic to peaked distributions would probably be gradual (possibly around 50 G).

Based on this scenario we propose PDFs here which are combinations of angle and field strength distributions. For the angular part we use the power law distribution introduced in Sect. 3, while for the field strength part we consider either a Voigt function (see Sect. 2.1) or a stretched exponential (see Sect. 2.2). The functional form of such a composite PDF is

$$P(y, \mu_B, \phi_B) d\mu_B d\phi_B dy = \frac{(p+1)}{2\pi} \begin{cases} P_V(y, a_B) \mu_B^p d\mu_B d\phi_B dy, \\ C e^{-|y|^k} \mu_B^p d\mu_B d\phi_B dy. \end{cases} \quad (5)$$

Here  $y$  varies in the range  $[-y_{\max}, +y_{\max}]$ ,  $\mu_B$  in the range  $[0, 1]$  and  $\phi_B$  in the range  $[0, 2\pi]$ .  $P_V(y, a_B)$  is given in Eq. (1). Asymmetric composite PDFs can be constructed by choosing different  $a_B$  (or  $k$ ) values for positive and

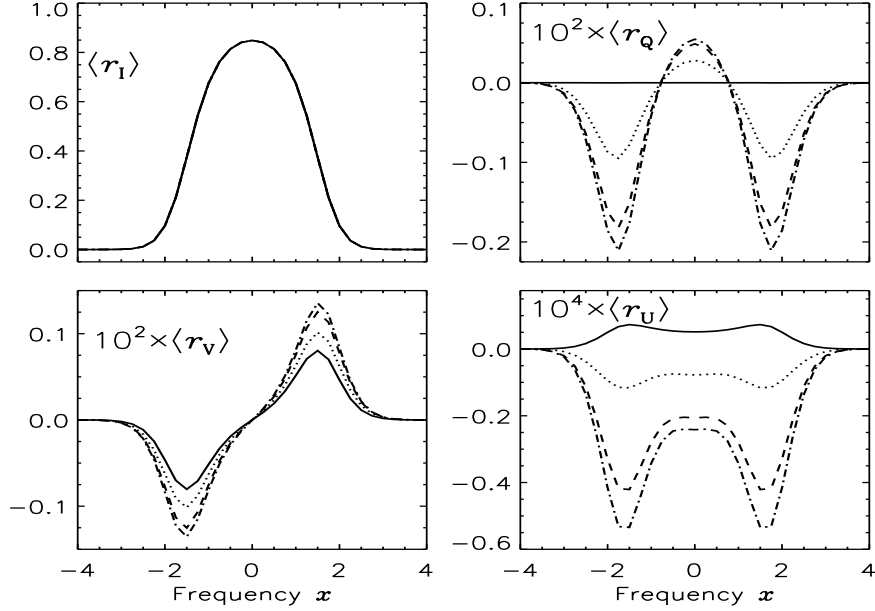


**Fig. 5.**  $\langle r_{I,Q,U,V} \rangle$  for  $\nu = 5$  and  $\mu = 0.1$ . Composite PDF containing asymmetric Voigt function with  $y_0 = 4.5$  (dashed line of Fig. 1a) is used. Line types are:  $y_t = \infty$  (solid),  $y_t = 50$  (dotted),  $y_t = 10$  (dashed), and  $y_t = 5$  (dash-dotted).

negative polarities of the Voigt (or stretched exponential). The angle and strength distributions are coupled by letting the power law index  $p$  depend on  $y$ . We have chosen  $p = |y|/y_t$  with  $y_t = B_t/\Delta_B$ , where  $B_t$  marks the transition between isotropic and peaked. Note that  $y_t = \infty$  corresponds to fully isotropic distribution for all field strengths.

We calculate mean residual Stokes parameters for the composite PDF containing an asymmetric Voigt with mean field  $y_0 = 4.5$  (dashed curve in Fig. 1a). The model parameters are  $(a, \beta, \gamma_B) = (0, 10, 0.0056)$  and  $\mu = 0.1$ . Figure 5 shows the solutions for  $\nu = 5$ . The different curve types correspond to different  $y_t$  values.  $\langle r_I \rangle$  is insensitive to the PDF asymmetry and to the variation of  $y_t$  due to the very weak value of  $\gamma_B$ . When  $y_t \rightarrow \infty$ , the PDF becomes fully isotropic, and hence  $\langle r_Q \rangle \rightarrow 0$ . As  $y_t$  decreases, the PDF becomes more and more anisotropic and hence  $\langle r_Q \rangle$  as well as  $\langle r_V \rangle$  increase in magnitude. In this case  $\langle r_U \rangle$  is generated through the magneto-optical effects. Therefore  $\langle r_U \rangle$  is very small, with a behavior similar to  $\langle r_Q \rangle$ .

## 5 Conclusions

We have presented mean Stokes profiles formed in media having spatially unresolved magnetic structures with sizes that are comparable to photon mean free

paths, using PDFs that describe fluctuations of the ambient field. A Gaussian PDF with isotropic or anisotropic fluctuations was considered in Frisch et al. (2005); here, we experimented with other types of PDFs with restriction to asymmetric PDFs which can generate non-zero net flux as diagnosed by the shape of  $\langle r_V \rangle$  profile. We consider very weak fluctuations of the magnetic field ( $\gamma_B = 0.0056$ ). Thus  $\langle r_I \rangle$  profiles remain insensitive to the shape of PDF. In contrast, other mean Stokes profiles are quite sensitive to the choice of PDF.

For a complete description of the random vector magnetic field we need PDFs which describe both the angular and strength fluctuations. We constructed such empirical PDFs by combining a power law (for angular distribution) with a Voigt function or a stretched exponential (for field strength). At the solar surface, weak fields are observed to be nearly isotropic and strong fields more vertical. Composite PDFs can simulate such a situation.

*Acknowledgement.* I am grateful to Dr. K. N. Nagendra for very useful suggestions and comments.

## References

- Carroll, T. A., Kopf, M. 2007, A&A, 468, 323  
 Carroll, T. A., Staude, J. 2003, Astronomische Nachrichten, 324, 392  
 Carroll, T. A., Staude, J. 2005, Astronomische Nachrichten, 326, 296  
 de Wijn, A. G., Stenflo, J. O., Solanki, S. K., Tsuneta, S. 2009, Space Sci. Rev. (in press)  
 Dolginov, A. Z., Pavlov, G. G. 1972, Soviet Astronomy, 16, 450  
 Domke, H., Pavlov, G. G. 1979, Ap&SS, 66, 47  
 Frisch, H., Sampoorna, M., Nagendra, K. N. 2005, A&A, 442, 11  
 Frisch, H., Sampoorna, M., Nagendra, K. N. 2006a, in Solar Polarization 4, eds. R. Casini & B. W. Lites, ASP Conf. Ser., 358, 126  
 Frisch, H., Sampoorna, M., Nagendra, K. N. 2006b, A&A, 453, 1095  
 Frisch, H., Sampoorna, M., Nagendra, K. N. 2007, Memorie della Societa Astronomica Italiana, 78, 142  
 Landi degl'Innocenti, E. 1994, in Solar Surface Magnetism, eds. R. J. Rutten & C. J. Schrijver, 29  
 Sampoorna, M., Frisch, H., Nagendra, K. N. 2008a, New Astronomy, 13, 233  
 Sampoorna, M., Nagendra, K. N., Frisch, H., Stenflo, J. O. 2008b, A&A, 485, 275  
 Stein, R. F., Nordlund, Å. 2006, ApJ, 642, 1246  
 Stenflo, J. O. 1987, Solar Phys., 114, 1  
 Stenflo, J. O., Holzreuter, R. 2002, in SOLMAG 2002. Proceedings of the Magnetic Coupling of the Solar Atmosphere Euroconference, ed. H. Sawaya-Lacoste, ESA Special Publication, 505, 101  
 Stenflo, J. O., Holzreuter, R. 2003a, in Current Theoretical Models and Future High Resolution Solar Observations: Preparing for ATST, eds. A. A. Pevtsov & H. Uitenbroek, ASP Conf. Ser., 286, 169  
 Stenflo, J. O., Holzreuter, R. 2003b, Astronomische Nachrichten, 324, 397  
 Vögler, A., Shelyag, S., Schüssler, M., et al. 2005, A&A, 429, 335